Adipocyte-specific FXR-deficiency protects adipose tissue from oxidative stress and insulin resistance and improves glucose homeostasis

Hélène Dehondt, Arianna Marino, Laura Butruille, Denis A Mogilenko, Arielle C Nzoussi Loubota, Oscar Chávez-Talavera, Emilie Dorchies, Emmanuelle Vallez, Joel Haas, Bruno Derudas, et al.

Original Article

MOLECULAR METABOLISM

Adipocyte-specific FXR-deficiency protects adipose tissue from oxidative stress and insulin resistance and improves glucose homeostasis

Hélène Dehondt [1,5], Arianna Marino [1,5], Laura Butruille [1,6], Denis A. Mogilenko [1,6,8], Arielle C. Nzoussi Loubota [1], Oscar Chávez-Talavera [1], Emilie Dorchies [1], Emmanuelle Vallez [1], Joel Haas [1], Bruno Derudas [1], Antonino Bongiovanni [2], Meryem Tardivel [2], Folkert Kuipers [3,4], Philippe Lefebvre [1], Sophie Lestavel [1], Anne Tailleux [1], David Dombrowicz [1], Sandrine Caron [1,*,7], Bart Staels [1,7]

ABSTRACT

Objective: Obesity is associated with metabolic dysfunction of white adipose tissue (WAT). Activated adipocytes secrete pro-inflammatory cytokines resulting in the recruitment of pro-inflammatory macrophages, which contribute to WAT insulin resistance. The bile acid (BA)-activated nuclear Farnesoid X Receptor (FXR) controls systemic glucose and lipid metabolism. Here, we studied the role of FXR in adipose tissue function.

Methods: We first investigated the immune phenotype of epididymal WAT (eWAT) from high fat diet (HFD)-fed whole-body FXR-deficient ($FXR^{-/-}$) mice by flow cytometry and gene expression analysis. We then generated adipocyte-specific FXR-deficient (Ad-$FXR^{-/-}$) mice and analyzed systemic and eWAT metabolism and immune phenotype upon HFD feeding. Transcriptomic analysis was done on mature eWAT adipocytes from HFD-fed Ad-$FXR^{-/-}$ mice.

Results: eWAT from HFD-fed whole-body $FXR^{-/-}$ and Ad-$FXR^{-/-}$ mice displayed decreased pro-inflammatory macrophage infiltration and inflammation. Ad-$FXR^{-/-}$ mice showed lower blood glucose concentrations, improved systemic glucose tolerance and WAT insulin sensitivity and oxidative stress. Transcriptomic analysis identified *Gsta4*, a modulator of oxidative stress in WAT, as the most upregulated gene in Ad-$FXR^{-/-}$ mouse adipocytes. Finally, chromatin immunoprecipitation analysis showed that FXR binds the *Gsta4* gene promoter.

Conclusions: These results indicate a role for the adipocyte FXR-GSTA4 axis in controlling HFD-induced inflammation and systemic glucose homeostasis.

Keywords White adipose tissue; Nuclear receptor FXR; Inflammation; Oxidative stress; Glucose metabolism

1. INTRODUCTION

Obesity increases the risk of type 2 diabetes and cardiovascular diseases [1]. Obesity is accompanied by chronic low-grade inflammation and predisposes to insulin resistance [2]. In an 'unhealthy' obesogenic context, white adipose tissue (WAT) expansion is accompanied by changes in the profile of adipocyte-secreted factors, impairing adipocyte differentiation, altering metabolic functions and inducing local inflammation in adipose tissue [3]. As a result, adipocytes become insulin resistant, which leads to increased lipolysis and altered membrane trafficking of the glucose transporter GLUT4 [3]. Local inflammation in fat develops as a result of the secretion of pro-inflammatory cytokines by the adipocytes [4], such as Tumor Necrosis Factor alpha (*Tnfα*) [5]. Adipose tissue inflammation, in turn, contributes to the recruitment of pro-inflammatory macrophages [6] and switches tissue resident anti-inflammatory macrophages to pro-inflammatory phenotypes [7]. These macrophage subsets also secrete pro-inflammatory cytokines, maintaining WAT inflammation and promoting local and systemic insulin resistance and glucose intolerance [5,8].

Metabolic diseases, such as obesity, are associated with qualitative and quantitative variations in the circulating bile acid (BA) pool [9,10].

[1]Univ. Lille, Inserm, CHU Lille, Institut Pasteur de Lille, U1011-EGID, F-59000 Lille, France [2]Univ. Lille, CNRS, Inserm, CHU Lille, Institut Pasteur de Lille, US 41 - UAR 2014 - PLBS, F-59000 Lille, France [3]Department of Laboratory Medicine, University Medical Center Groningen, University of Groningen, Groningen, the Netherlands [4]Department of Pediatrics, University Medical Center Groningen, University of Groningen, Groningen, the Netherlands

[5] Both co-first authors contributed equally to this work.
[6] Both co-second authors contributed equally to this work.
[7] Co-last authors.
[8] Present address: Department of Medicine, Department of Pathology, Microbiology, and Immunology, Vanderbilt Center for Immunobiology, Vanderbilt University Medical Center, Nashville, TN, USA.

*Corresponding author. UMR1011 INSERM-Université de Lille. Pôle Recherche. Bâtiment J&K. Boulevard du Pr Leclerc. 59045 Lille Cedex. France. E-mail: sandrine.caron-houde@univ-lille.fr (S. Caron).

Received December 20, 2022 • Accepted January 29, 2023 • Available online 4 February 2023

https://doi.org/10.1016/j.molmet.2023.101686

BA are detergent molecules promoting lipid emulsification and absorption in the intestine. BA, however, also act as signaling molecules, activating, amongst others, the nuclear receptor Farnesoid X Receptor (FXR, NR1H4) [9]. FXR, which is highly expressed in the liver and intestine, regulates the synthesis and enterohepatic cycling of BA and systemic glucose and lipid metabolism [10–12]. Interestingly, several studies have suggested that FXR also controls whole-body energy metabolism. Indeed, whole-body FXR-deficient mice are protected from diet- and genetically-induced obesity and display reduced adiposity. In contrast, liver-specific FXR-deficiency does not protect mice from HFD-induced obesity [13], suggesting a role for FXR in peripheral tissues. In line, FXR is expressed in WAT and regulates the *in vitro* differentiation of pre-adipocytes into adipocytes [14–16]. Moreover, FXR-deficiency alters adipocyte function by enhancing lipolysis and decreasing lipogenesis [16].

To further characterize the role of FXR in adipose tissue function, we first studied the response of whole-body FXR-deficient mice to a HFD. We observed decreased WAT inflammatory macrophage infiltration and decreased expression of inflammatory genes in both fat macrophages and adipocytes. To further delineate the role of FXR in adipocytes, we next developed an adipocyte-specific FXR-deficient mouse model (Ad-FXR$^{-/-}$). Whereas adipocyte-specific FXR-deficiency did not result in differences in body weight upon HFD feeding, Ad-FXR$^{-/-}$ mice displayed lower blood glucose concentrations and improved systemic glucose tolerance and WAT insulin sensitivity. In line, inflammatory macrophage infiltration, as well as the expression of inflammatory genes, were reduced in the WAT of Ad-FXR$^{-/-}$ mice. Transcriptomic analysis identified *Gsta4*, an antioxidant enzyme, as the most upregulated gene in Ad-FXR$^{-/-}$ adipocytes, hence providing a potential mechanism contributing to the decreased WAT inflammation, the increased WAT insulin sensitivity and systemic glucose tolerance upon adipocyte-specific FXR-deficiency.

2. RESULTS

2.1. FXR$^{-/-}$ mice are protected from high fat diet (HFD)-induced obesity and adipose tissue inflammation

To investigate the potential role of FXR in white adipose tissue (WAT) function, whole-body FXR$^{-/-}$ and FXR$^{+/+}$ littermate mice were fed a HFD for 12 weeks. As observed previously [13], FXR$^{-/-}$ mice were protected from HFD—induced obesity and fasting hyperglycemia (Supp. Figure 1A&B). This protection from HFD-induced obesity in FXR$^{-/-}$ mice correlated with a significantly reduced weight of epididymal (eWAT) and inguinal (iWAT) WAT (Supp. Figure 1C). Since HFD-induced obesity is accompanied by WAT inflammation [3], we next investigated the inflammatory phenotype of FXR$^{-/-}$ eWAT by flow cytometry analysis (Supp. Figure 2; details in 'Materials and Methods' Section 4.2). Whereas no difference was observed between the two genotypes when fed a low fat diet (LFD), HFD feeding resulted in the expected increase in macrophage (CD45^{+}CD11b^{+}F4/80^{+} cells) proportions and numbers in eWAT from FXR$^{+/+}$ compared to FXR$^{-/-}$ mice (Figure 1A). Moreover, HFD-fed FXR$^{-/-}$ mice displayed a significantly lower proportion of pro-inflammatory macrophages (CD45^{+} CD11b^{+} F4/80^{+} CD11c^{+} CD206^{-} cells) (Figure 1B, *left*) and a higher proportion of anti-inflammatory macrophages (CD45^{+} CD11b^{+} F4/80^{+} CD11c^{-} CD206^{+} cells) (Figure 1B, *middle*), resulting in a lower ratio of pro-/anti-inflammatory macrophages in eWAT (Figure 1B, *right*). These results indicate that the HFD-induced pro-inflammatory polarization of eWAT macrophages is significantly reduced in FXR$^{-/-}$ mice. In line, gene expression levels of *Adgre1* (*F4/80*), expressed by all macrophages, *Itgax* (*Cd11c*), expressed by myeloid cells, and *Cd64*, expressed more specifically by pro-inflammatory monocytes and macrophages, were not induced by HFD-feeding in eWAT of FXR$^{-/-}$ mice. At the same time, HFD feeding strongly increased the expression levels of these markers in FXR$^{+/+}$ mice (Figure 1C). No alteration of *Ccr2* gene expression, the receptor for the monocyte chemokine CCL2, was found in eWAT from FXR$^{-/-}$ mice (Figure 1C). Since no differences in macrophage subsets were observed between LFD-fed FXR$^{+/+}$ and FXR$^{-/-}$ mice, we further focused on HFD-fed mice. eWAT from HFD-fed FXR$^{-/-}$ mice showed significantly reduced mRNA levels of *Tnfα* and *Il6*, whereas *Il1β* mRNA levels were not different (Figure 1D). These results show that FXR-deficiency reduces HFD-induced adipose tissue inflammation.

2.2. Both adipose tissue macrophages and mature adipocytes display reduced inflammatory gene expression in HFD-fed FXR$^{-/-}$ mice

To determine the potential contribution of adipocytes and macrophages to the reduced inflammation in eWAT of HFD-fed FXR$^{-/-}$ mice, mature adipocytes and macrophages were isolated from eWAT of HFD-fed FXR$^{+/+}$ and FXR$^{-/-}$ mice. eWAT macrophages from FXR$^{-/-}$ mice showed lower expression levels of *Tnfα* and (although borderline significant) *Il6* (Figure 2A), whereas *Il1β* gene expression levels were not different. Interestingly, expression levels of *Tnfα*, *Il6* and *Il1β* were lower in FXR$^{-/-}$ compared to FXR$^{+/+}$ adipocytes (Figure 2B, *top*). Mature FXR$^{-/-}$ adipocytes also showed higher *aP2* (*Fabp-4*) and adiponectin (*AdipoQ*) expression levels (Figure 2B, *bottom*).

2.3. Adipocyte-specific FXR-deficiency protects mice from HFD-induced hyperglycemia and eWAT insulin resistance

Since we found that FXR protein and mRNA are expressed in WAT in adipocytes (Supp. Figure 3A,C), but not in WAT macrophages (*data not shown*), we next determined the role of adipocyte FXR by creating an adipocyte-specific FXR-deficient mouse model (Ad-FXR$^{-/-}$). Therefore, FXR-floxed (FXR$^{fl/fl}$) mice [17] were crossed with mice expressing the Cre-recombinase under the control of the adiponectin promoter (adiponectin-Cre^{+} mice) [18] (See Appendix A and Supp. Figure 3 for details on the mouse model generation and validation). In these mice, *Fxr* expression was decreased specifically in adipocytes (Supp. Figure 3). Ad-FXR$^{-/-}$ and Ad-FXR$^{+/+}$ littermate mice displayed similar weight gain on LFD and HFD diets (Figure 3A) and similar eWAT and iWAT weights (Supp. Figure 4A). Ad-FXR$^{+/+}$ and Ad-FXR$^{-/-}$ mice did not show differences in fasting glycemia when fed a LFD (*data not shown*). By contrast, compared to Ad-FXR$^{+/+}$ mice, Ad-FXR$^{-/-}$ mice showed significantly lower fasting blood glucose levels after 7 and 11 weeks of HFD feeding (Figure 3B), whereas fasting serum insulin levels were not different at 12 weeks (Figure 3C). Moreover, intra-peritoneal glucose tolerance tests (IPGTT) showed no difference between LFD-fed Ad-FXR$^{-/-}$ and Ad-FXR$^{+/+}$ littermate mice, whereas HFD-fed Ad-FXR$^{-/-}$ displayed significantly improved glucose tolerance compared to Ad-FXR$^{+/+}$ mice (Figure 3D). Whole-body insulin sensitivity, measured by insulin tolerance test (ITT), tended to be increased in Ad-FXR$^{-/-}$ compared to Ad-FXR$^{+/+}$ mice (Supp. Figure 4B). To determine whether adipose tissue insulin sensitivity was affected, insulin was intraperitoneally injected in Ad-FXR$^{-/-}$ and control littermate mice fed a HFD for 12 weeks and the Akt phosphorylation levels in eWAT were assessed. eWAT Akt phosphorylation was more pronouncedly increased by insulin in Ad-FXR$^{-/-}$ compared to Ad-FXR$^{+/+}$ mice (Figure 3E). In line, histological analysis showed that the population of smaller adipocytes, which generally are more insulin sensitive than lipid-laden hypertrophic adipocytes, was enriched in eWAT of Ad-FXR−/− vs Ad-FXR+/+ mice on high omega-6 HFD (Supp. Figure 5).

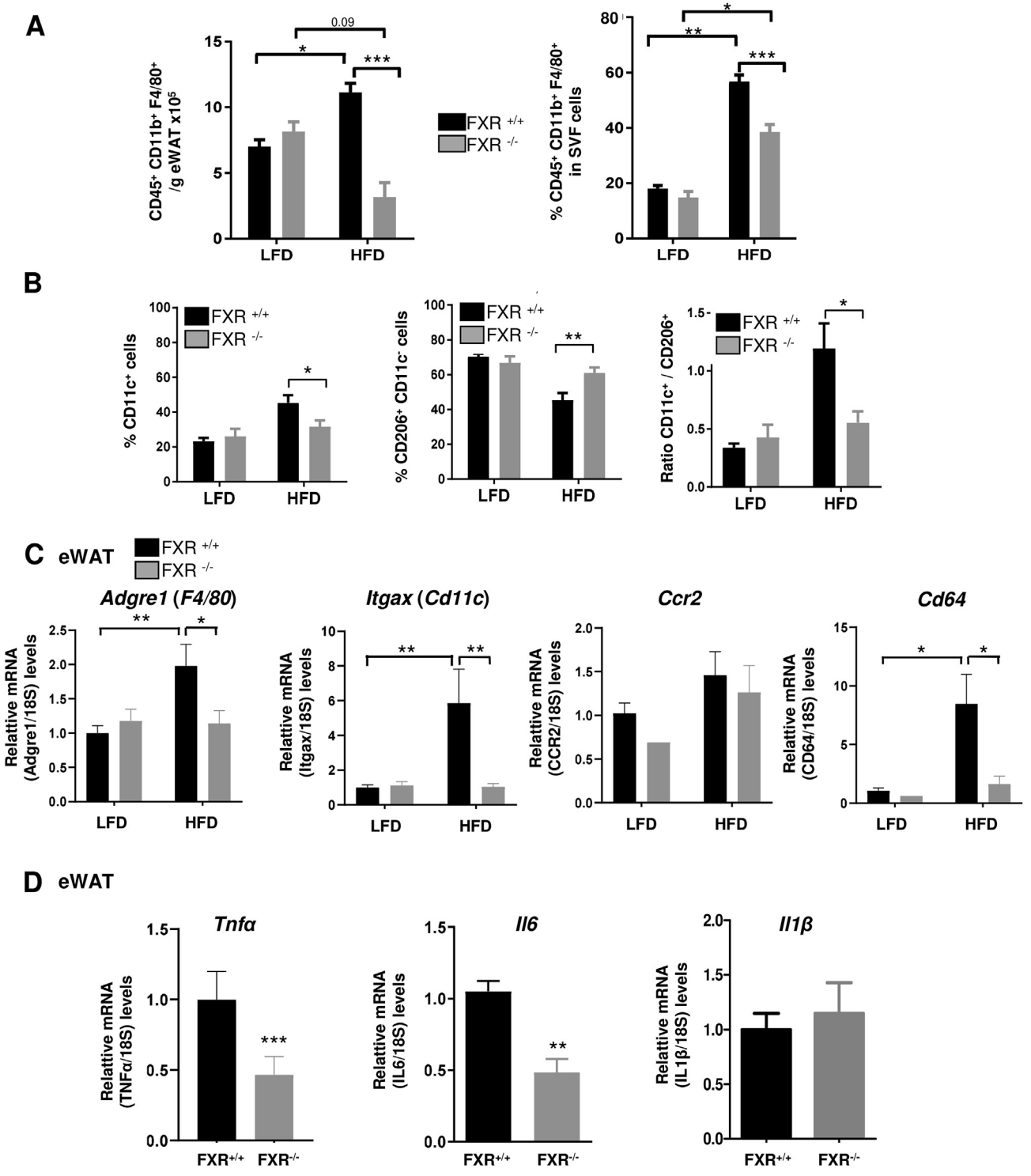

Figure 1: FXR$^{-/-}$ mice are protected from HFD-induced macrophage infiltration and inflammation in eWAT. eWAT from FXR$^{-/-}$ and FXR$^{+/+}$ mice fed LFD or HFD for 12 weeks were analyzed. (A) Macrophage (CD45$^+$ F4/80$^+$ CD11b$^+$) absolute number expressed per gram of eWAT (left) and the proportion of total CD45$^+$ immune cells in the stromal vascular fraction (SVF) (right) was evaluated by flow cytofluorimetry analysis. (B) Pro-inflammatory (CD45$^+$ F4/80$^+$ CD11b$^+$ CD11c$^+$; indicated 'CD11c$^+$') (left), anti-inflammatory (CD45$^+$ F4/80$^+$ CD11b$^+$ CD11c$^-$CD206$^+$; indicated 'CD206$^+$ CD11c$^-$') (middle) profile macrophage number expressed as % of total macrophages (CD45$^+$ F4/80$^+$ CD11b$^+$) were analyzed by flow cytofluorimetric analysis; ratio of pro-inflammatory (CD11c$^+$)/anti-inflammatory (CD206$^+$ CD11c$^-$) (right) profile macrophage number. Expression of *adgre1* (F4/80), Itgax (Cd11c), Ccr2, Cd64 macrophage markers (C) and of inflammatory genes (D) was evaluated by qPCR in eWAT, normalized to *18S* and expressed relative to those of FXR$^{+/+}$ mice on LFD (C) or HFD (D). The results shown are the pool of results obtained from two independent experiments (LFD, n = 4 per genotype; HFD, n = 8-9 per genotype). Values are expressed as mean ± SEM; $*p < 0.05$, $**p < 0.01$, $***p < 0.001$. Statistical significances are determined by two-way ANOVA with Tukey *post-hoc* test.

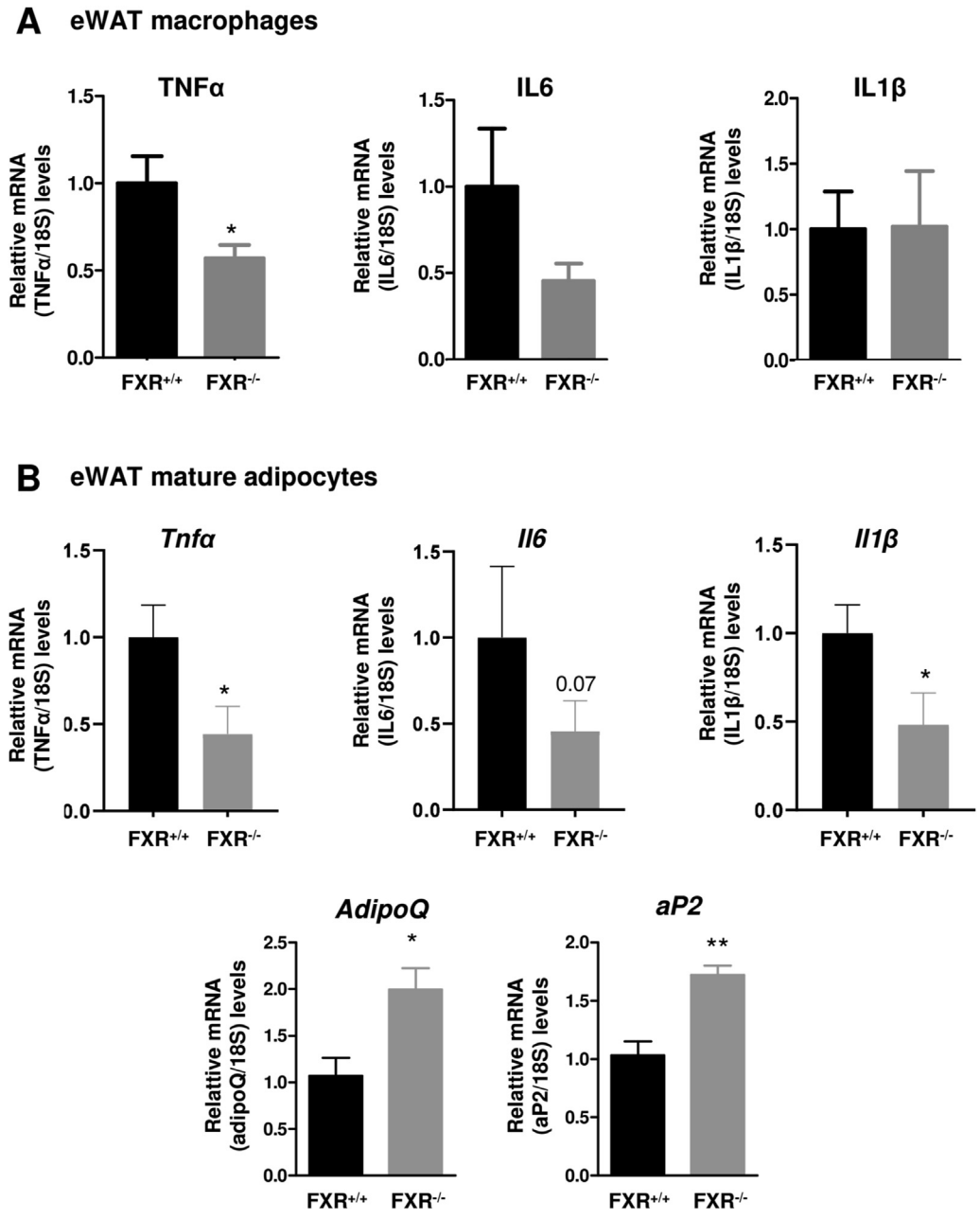

Figure 2: Inflammatory gene expression is decreased in WAT macrophages and mature adipocytes of FXR$^{-/-}$ mice on HFD. Gene expression in macrophages (A) and mature adipocytes (B) from eWAT of FXR$^{-/-}$ and FXR$^{+/+}$ mice fed a HFD for 12 weeks was analyzed by qPCR, normalized to 18S and expressed relative to those of FXR$^{+/+}$ mice on HFD. The results shown are the pool of results obtained from two independent experiments (HFD, n = 8-9 per genotype). Values are expressed as mean ± SEM; $*p < 0.05$, $**p < 0.01$. Statistical significances are determined by student's t-test.

Taken together, these results indicate that, whereas adipocyte FXR-deficiency does not modify HFD-induced obesity, fasting plasma glycemia, the response of WAT to insulin and whole-body glucose homeostasis are improved in Ad-FXR$^{-/-}$ mice.

2.4. Adipocyte-specific FXR-deficiency protects against HFD-induced adipose tissue inflammation

Since whole-body FXR-deficiency strongly affected HFD-induced adipose tissue inflammation, we next assessed the inflammatory status of adipose tissue in HFD-fed Ad-FXR$^{-/-}$ and Ad-FXR$^{+/+}$ littermate mice by flow cytometry analysis (Supp. Figure 2; details in 'Materials and Methods' Section 4.2). Similar to in whole-body FXR-deficient mice (Figures 1 and 2), no difference was observed in immune cell content nor inflammation in eWAT of LFD-fed mice. Whereas HFD feeding induced eWAT macrophage infiltration to the same extent in both genotypes (Figure 4A), HFD-fed Ad-FXR$^{-/-}$ mice displayed a significantly lower proportion of pro-inflammatory CD11c^{+} macrophages (Figure 4B, *left*), whereas the proportion of macrophages with an anti-inflammatory phenotype (CD11c^{-} CD206^{-}) was not altered (Figure 4B, *middle*). As a result, a significantly lower ratio of pro-/anti-inflammatory macrophages was observed in Ad-FXR$^{-/-}$ compared to Ad-FXR$^{+/+}$ littermate mice (Figure 4B, *right*). In line, eWAT mRNA levels of

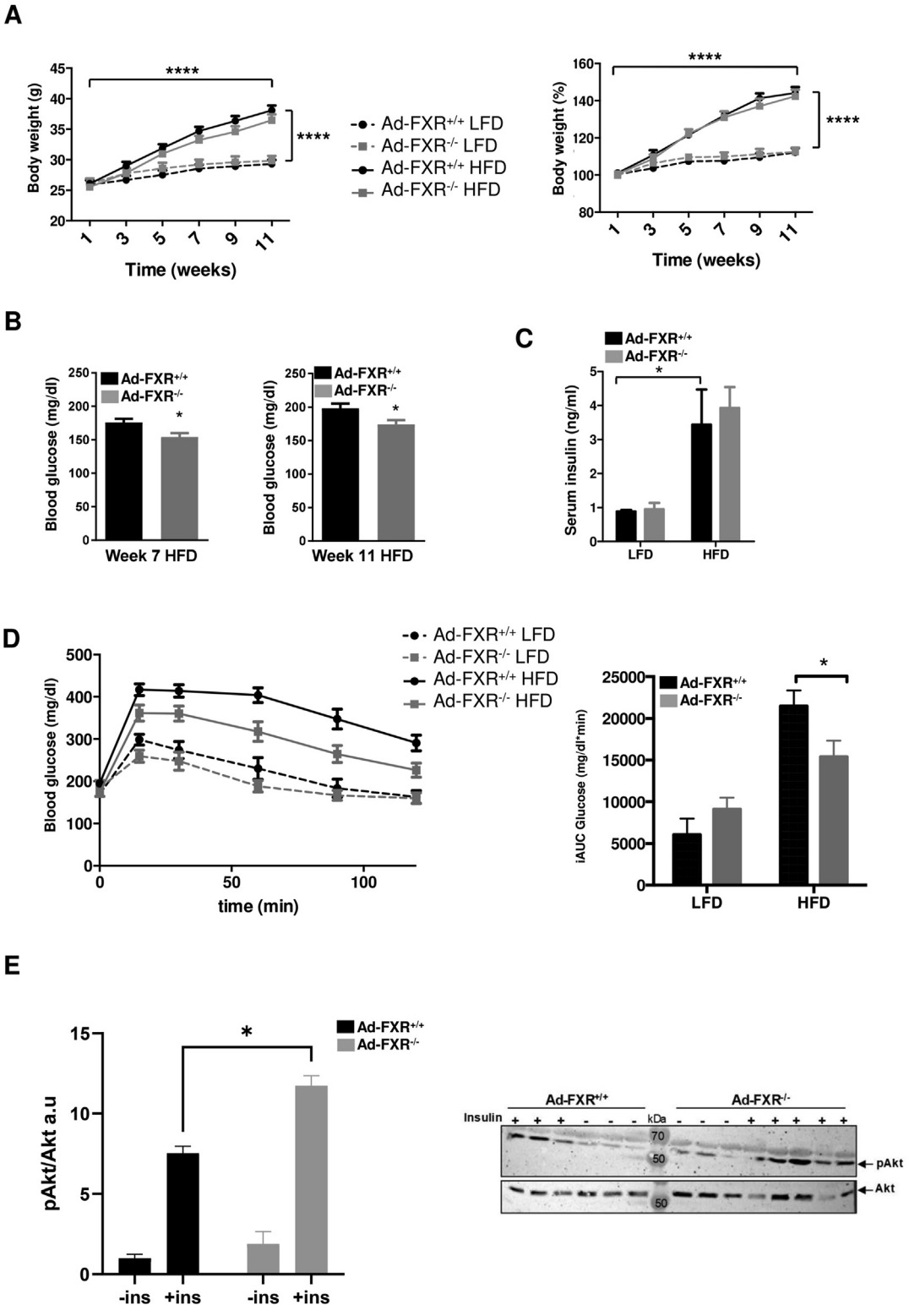

Figure 3: Adipocyte (Ad)-FXR$^{-/-}$ mice are protected from HFD-induced hyperglycemia and eWAT insulin resistance. Ad-FXR$^{-/-}$ mice and Ad-FXR$^{+/+}$ were fed a LFD or a HFD for 12 weeks. (A) Body weight expressed in gram (left) and as % of body weight increase (right). (B) Fasting glycemia at 7 and 11 weeks of diet. (C) Serum fasting insulin at 12 weeks of diet. (D) Blood glucose excursion curves (left) and integrated AUC values (right) after administration of an intraperitoneal glucose bolus (IPGTT; 1 g/kg glucose) were measured at the end of the feeding period. The results shown (A, B, C, D) are the pool of results obtained from three independent experiments (LFD, n = 10-11 per genotype; HFD, n = 16-21 per genotype). Values are expressed as mean ± SEM; $*p < 0.05$, $**p < 0.01$. Statistical significances are determined by two-way ANOVA with Tukey *post-hoc* test or student's t-test. (E) Phospho-Akt (pAkt; Ser473) and Akt protein levels in eWAT after intraperitoneal injection of insulin in HFD-fed Ad-FXR$^{+/+}$ and Ad-FXR$^{-/-}$ mice. Protein levels were evaluated by Western blot and quantified. The samples (n = 3-5 per genotype (3 for the two groups without insulin and for the group 'Ad-FXR$^{+/+}$ with insulin'; 5 for the group 'Ad-FXR$^{-/-}$ with insulin) were analyzed simultaneously on the same gel. The quantification was performed with all the samples (left) and the western blot result is shown (right).

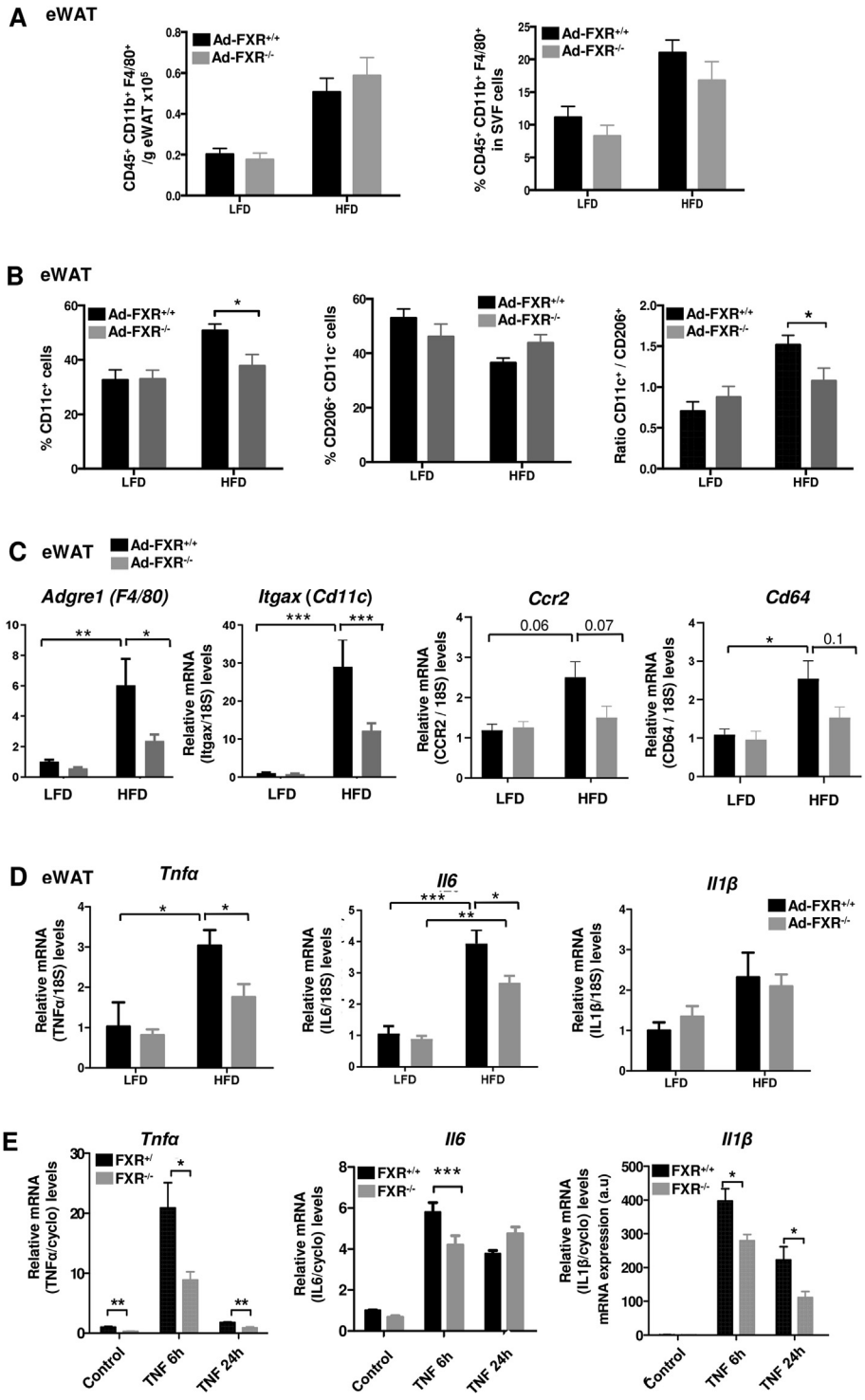

Figure 4: Ad-FXR$^{-/-}$ mice display decreased HFD-induced pro-inflammatory macrophage infiltration and inflammation in eWAT. eWAT from Ad-FXR$^{-/-}$ and Ad-FXR$^{+/+}$ mice fed LFD or HFD for 12 weeks was analyzed. (A) Macrophage (CD45$^+$ F4/80$^+$ CD11b$^+$) absolute number expressed per gram of eWAT (left) and the proportion of total CD45$^+$ immune cells in the stromal vascular fraction (right) was evaluated by flow cytofluorimetry analysis. (B) Pro-inflammatory (CD45$^+$ F4/80$^+$ CD11b$^+$ CD11c$^+$; indicated 'CD11c^{++}') (left), anti-inflammatory (CD45$^+$ F4/80$^+$ CD11b$^+$ CD206$^+$ CD11c$^-$; indicated 'CD206$^+$ CD11c^{++}') (middle) profile macrophage number expressed as % of total macrophages (CD45$^+$ F4/80$^+$ CD11b$^+$) were analyzed by flow cytofluorimetric analysis; ratio of pro-inflammatory (CD11c$^+$)/anti-inflammatory (CD206$^+$ CD11c$^-$) (right) profile macrophage number. Expression of adgre1 (F4/80), Itgax (Cd11c), Ccr2, Cd64 macrophage markers (C) and of inflammatory gene (D) was evaluated by qPCR in eWAT. The expression levels were normalized to 18S and expressed relative to those of Ad-FXR$^{+/+}$ mice on LFD. The results shown are the pool of results obtained from three experiments performed in an independent manner (LFD, n = 10/genotype; HFD, n = 16/genotype). Values are expressed as mean ± SEM; *$p < 0.05$. Statistical significances are determined by two-way ANOVA with Tukey *post-hoc* test. (E) FXR$^{+/+}$ and FXR$^{-/-}$ pre-adipocytes were differentiated in vitro for 8 days and stimulated for 6h and 24h with *Tnfα* (20 ng/ml). Inflammatory gene expression was analyzed by qPCR. Gene expression was normalized to *cyclophilin A* and expressed relative to those of FXR$^{+/+}$ primary adipocytes without cytokine treatment. Values are expressed as mean ± SD; *$p < 0.05$, **$p < 0.01$, ***$p < 0.001$. Statistical significances are determined by two-way ANOVA with Tukey *post-hoc* test.

Adgre1 (*F4/80*), *Itgax* (*Cd11c*), *Cd64* as well as *Ccr2* were also lower in Ad-FXR$^{-/-}$ compared to Ad-FXR$^{+/+}$ littermate mice (Figure 4C). Finally, the gene expression levels of *Tnfα* and *Il6*, but not *Il1β* were lower in eWAT from HFD-fed Ad-FXR$^{-/-}$mice (Figure 4D). These results indicate that adipocyte FXR-deficiency contributes to the protection of eWAT from HFD-induced inflammation.

To determine if the effect of adipocyte FXR on the inflammatory response was cell-autonomous, stromal vascular fraction (SVF) cells were isolated from FXR$^{+/+}$ and FXR$^{-/-}$ eWAT and the response of *in vitro* differentiated adipocytes to the pro-inflammatory cytokine *Tnfα* was assessed [5,8]. *In vitro* differentiation of pre-adipocytes resulted in the induction of the adipocyte marker gene *Adiponectin* (Supp. Figure 6), which was less pronounced in FXR$^{-/-}$ than in FXR$^{+/+}$ adipocytes. FXR$^{-/-}$ adipocytes displayed lower *Tnfα*-induced *Tnfα*, *Il6* and *Il1β* mRNA levels (Figure 4E), indicating that adipocyte FXR-deficiency results in a cell-intrinsic diminished inflammatory response.

2.5. Adipocyte-specific FXR-deficiency protects eWAT from HFD-induced oxidative stress

To unravel the mechanisms underlying the reduced inflammation in adipose tissue of Ad-FXR$^{-/-}$ mice, a transcriptomic analysis of mature adipocytes isolated from eWAT of HFD-fed Ad-FXR$^{-/-}$ and Ad-FXR$^{+/+}$ mice was performed (Figure 5A). In line with the previous findings, the expression level of inflammatory genes was generally lower (Figure 5B), whereas xenobiotic metabolism genes were higher expressed in FXR$^{-/-}$ adipocytes (Figure 5C). An enrichment in genes involved in adipocyte function (Figure 5D) and insulin signaling (Figure 5E) was observed in FXR$^{-/-}$ adipocytes, which is in line with the improved eWAT insulin sensitivity (Figure 3E).

Interestingly, *Gsta4*, a Glutathione S-transferase family member, was the most differentially expressed gene between adipocytes of both genotypes (Figure 5A). *Gsta4* is an anti-oxidant enzyme which catalyzes the glutathionylation of trans-4-hydroxy-2-nonenal (4-HNE), a lipid peroxidation end-product and marker of oxidative damage. The enzymatic activity of *Gsta4* produces conjugated 4-HNE products [19]. In adipose tissue, down-regulation of *Gsta4* gene expression has been shown to increase oxidative stress [20,21]. Whereas HFD feeding decreased *Gsta4* expression in both genotypes (Supp. Figure 4C), both *Gsta4* mRNA (*left*) and protein (*right*) levels were higher in eWAT of HFD-fed Ad-FXR$^{-/-}$ mice (Figure 6A). In line with the HFD-induced decrease of *Gsta4* expression, HFD feeding resulted in elevated 4-HNE levels in Ad-FXR$^{+/+}$ eWAT (*data not shown*). Interestingly, 4-HNE levels were significantly lower in eWAT of HFD-fed Ad-FXR$^{-/-}$ compared to Ad-FXR$^{+/+}$ mice (Figure 6B). In line, analysis of protein carbonylation showed that eWAT of Ad-FXR−/− mice displayed lower levels of carbonylation than eWAT of Ad-FXR+/+ mice fed a high omega-6 HFD (Supp. Figure 7), indicative of lower oxidative stress. Moreover, *in vitro* differentiated FXR$^{-/-}$ adipocytes expressed higher mRNA levels of *Gsta4* (Figure 6C). These results show that adipocyte FXR-deficiency results in an induction of *Gsta4* expression, associated with a decreased HFD-induced oxidative stress in eWAT.

To assess whether *Gsta4* may be directly regulated by FXR, mouse liver chromatin-immunoprecipitation-sequencing (ChIP-seq) datasets were assessed and revealed the presence of FXR binding sites on the *Gsta4* promoter [22] (http://genome.ucsc.edu/goldenPath/customTracks/custTracks.html#Mouse). In line, ChIP qPCR analysis revealed FXR protein binding to the *Gsta4* gene promoter in FXR$^{+/+}$ but not in FXR$^{-/-}$ adipocytes (Figure 6D), suggesting that *Gsta4* is a direct FXR target gene.

3. DISCUSSION

In this study, we show that whole-body FXR-deficient mice display a decreased pro-inflammatory macrophage infiltration and inflammation in eWAT when fed a HFD. Using Ad-FXR$^{-/-}$ mice, we found that this phenotype is partially mediated by adipocyte-expressed FXR. Ad-FXR$^{-/-}$ mice further displayed improved glucose homeostasis, associated with an improved WAT insulin sensitivity and lower inflammation. The identification of the anti-oxidant enzyme *Gsta4* as the most strongly induced gene in FXR-deficient adipocytes and its potential direct regulation by FXR provides a plausible contributing mechanism to explain the decreased WAT inflammation and improved systemic glucose homeostasis.

In contrast to the body weight changes, at least a part of the regulation of WAT inflammation by FXR is linked to adipocytes, since both FXR$^{-/-}$ and Ad-FXR$^{-/-}$ mice displayed a decreased inflammation profile. The effect of FXR on inflammation is adipocyte autonomous since *in vitro* differentiated FXR-deficient adipocytes showed a reduced response to stimulation with *Tnfα*, a primary HFD-induced cytokine [5,8]. So far, the involvement of the nuclear receptor FXR in WAT function has received little attention and the role of adipocyte FXR in WAT inflammation has not been described. One study showed that treatment of HFD-fed rats with chenodeoxycholic acid (CDCA), an endogenous FXR ligand, decreased pro-inflammatory cytokine levels in WAT [24]. Still, neither the role of FXR nor the tissues targeted by CDCA, were identified. Other studies showed that FXR activation decreases macrophage activation and inflammation in the liver [25–28], intestine [29–31] and stomach [32] in mouse and human. Our results clearly show a pro-inflammatory role of adipocyte FXR, since its deletion promotes decreased HFD-induced WAT inflammation, an apparent contradiction with the reported anti-inflammatory effect of FXR in other tissues.

Interestingly, both results obtained in FXR$^{-/-}$ and Ad-FXR$^{-/-}$ mice fed a HFD reveal that not only the whole-body, but also adipocyte-specific FXR-deficiency, results in decreased pro-inflammatory macrophage infiltration and inflammation. This effect was more pronounced in whole-body FXR$^{-/-}$ mice probably because of the lower HFD-induced body weight gain combined with actions of FXR in other cell types, present in eWAT or other tissues. Indeed, FXR is also expressed in endothelial cells [11] and macrophages in certain tissues [24,33], in which FXR might contribute to elevated inflammation levels upon HFD-induced obesity [2]. However, we were not able to detect the expression of FXR in WAT macrophages (*data not shown*). Nevertheless, the expression of surface markers of inflammation and inflammation-related cytokines was also lower in eWAT macrophages from HFD-fed Ad-FXR$^{-/-}$ mice, which suggests the contribution of other WAT cells, probably adipocytes, to this macrophage phenotype. It is known that adipocytes also contribute to obesity-induced inflammation [34]. Thus, adipocytes can produce pro-inflammatory cytokines and lipids promoting pro-inflammatory macrophage recruitment and a switch of resident anti-inflammatory to pro-inflammatory macrophages [6,7,35]. Adipocyte-specific FXR deficiency likely reduces the secretion of pro-inflammatory cytokines and subsequent pro-inflammatory macrophage infiltration and phenotypic switch of resident macrophages. In line, transgenic mice that overexpress human FXR in adipocytes display fibrosis, often associated with inflammation development [36].

The decrease in eWAT inflammatory macrophage number correlates with an improvement of eWAT insulin sensitivity, indicating a paracrine

A

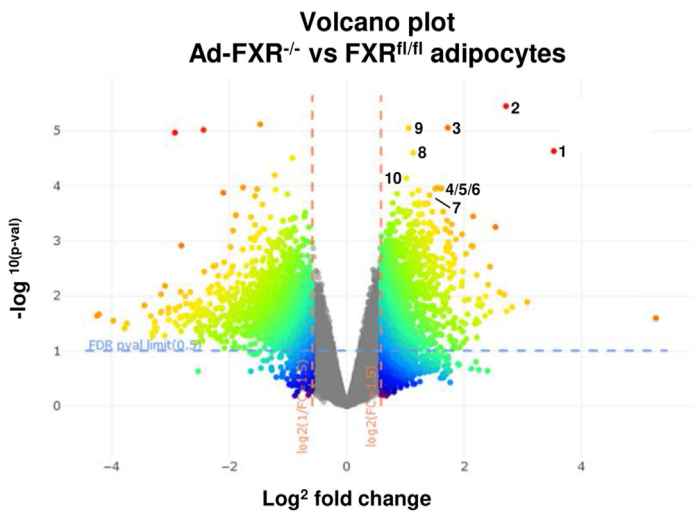

	Gene	Fold change	p-value
1	*Gsta4*	11.520	2.330 *10^{-5}
2	*Bckdhb*	6.560	3.549 *10^{-6}
3	*Arxes2*	3.300	8.769 *10^{-6}
4	*Aspa*	3.060	1.110 *10^{-4}
5	*Fitm2*	2.922	1.078 *10^{-4}
6	*Arxes1*	2.844	1.129 *10^{-4}
7	*Rgs7*	2.665	1.470 *10^{-4}
8	*Gca*	2.195	2.497 *10^{-5}
9	*L3hypdh*	2.079	8.902 *10^{-6}
10	*Clpx*	2.023	7,257 *10^{-5}

B

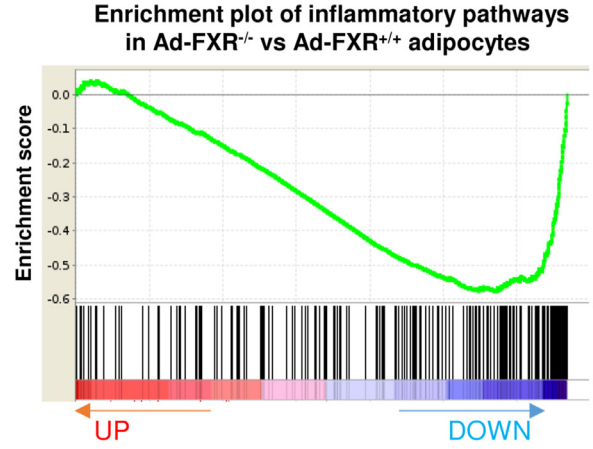

C

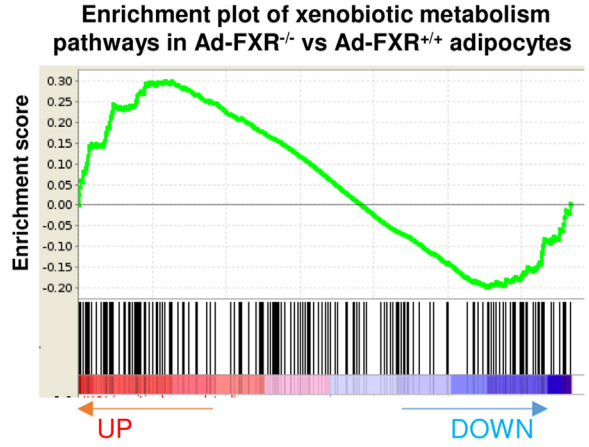

D

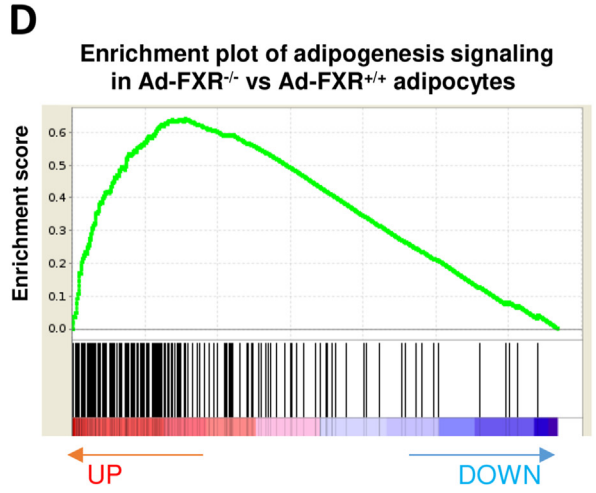

E

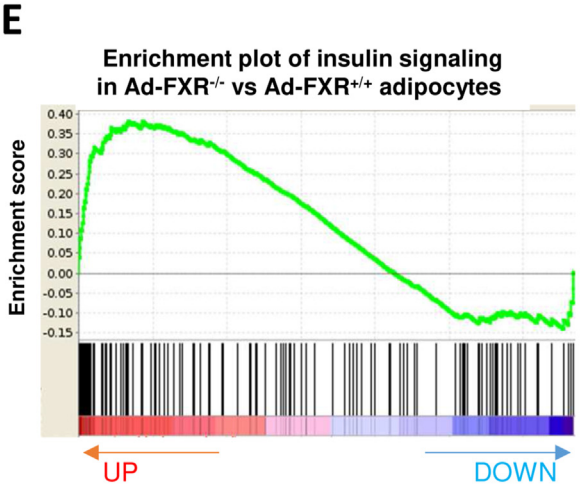

Figure 5: Adipocytes from Ad-FXR$^{-/-}$ mice display increased glutathione S-transferase alpha 4 (*Gsta4*) gene expression. Ad-FXR$^{-/-}$ and Ad-FXR$^{+/+}$ mice were fed a HFD for 12 weeks. DNA microarray analysis was performed using mRNA from mature adipocytes (n = 5 per genotype). (A) Volcano-plot of transcriptomic analysis (the numbers correspond to the 10 most differentially expressed genes listed in the table) (left); list of the 10 most differentially expressed genes in mature adipocytes of Ad-FXR$^{-/-}$ mice versus mature adipocytes of Ad-FXR$^{+/+}$ (right) (fold change and p-value were indicated) Gene Set Enrichment Analysis (GSEA) for inflammatory signaling (B), xenobiotic metabolism (C), adipogenesis signaling function (D) and insulin signaling (E) gene sets.

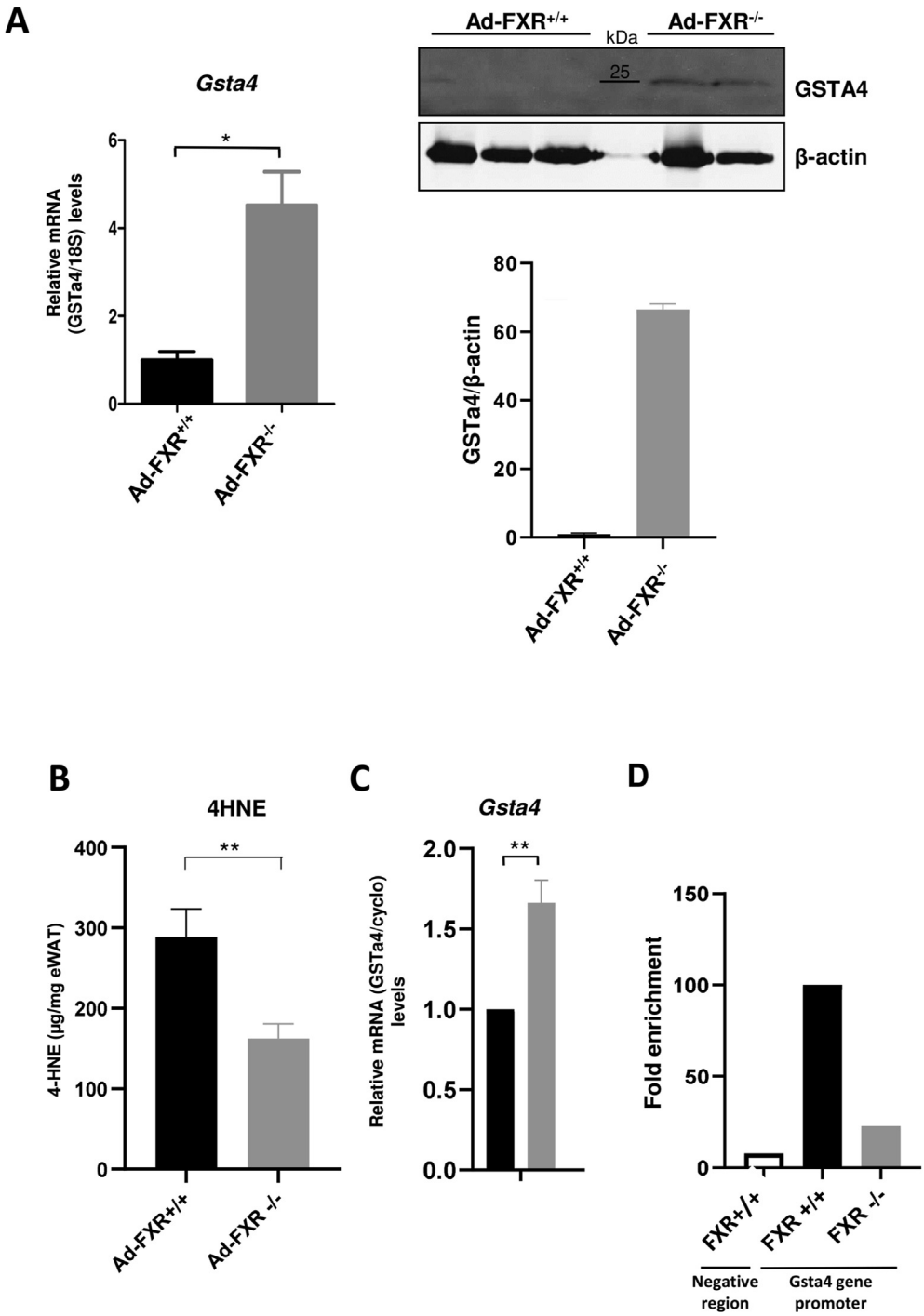

Figure 6: FXR-deficiency induces *Gsta4* gene expression upregulation (A) *Gsta4* gene (left), *Gsta4* protein (right) and (B) 4HNE levels were analyzed in eWAT from Ad-FXR$^{+/+}$ and Ad-FXR$^{-/-}$ mice fed a LFD and a HFD by qPCR, Western blot and ELISA, respectively. qPCR gene expression was normalized to 18S and expressed relative to Ad-FXR$^{+/+}$ mice on LFD. Values are expressed as mean ± SEM. Statistical significances are determined by two-way ANOVA with Tukey *post-hoc* test or student's t-test. For Western blot analysis, samples were run and analyzed simultaneously on a single gel. (C) FXR$^{+/+}$and FXR$^{-/-}$ primary adipocytes were differentiated in vitro for 8 days. *Gsta4* gene expression was analyzed by qPCR, normalized to *Cyclophilin A* and expressed relative to those of FXR$^{+/+}$ primary adipocytes without cytokine treatment. Values are expressed as mean ± SD; $*p < 0.05$, $**p < 0.01$. Statistical significances are determined by two-way ANOVA with Tukey *post-hoc* test or student's t-test. (D) FXR binding on a negative control region and the *Gsta4* gene promoter after Chromatin Immunoprecipitation (ChIP) of in vitro FXR$^{+/+}$ and FXR$^{-/-}$ differentiated adipocytes using a FXR specific antibody. The fold enrichment was quantified by qPCR using specific primers covering the negative control (a region in the genome with no transcription regulation mark and used to define the experiment background) and FXRE regions in the *Gsta4* promoter. The FXR fold enrichment on the *Gsta4* gene promoter in the FXR$^{+/+}$ differentiated adipocytes was arbitrarily set to 100.

improvement of local tissue metabolism [5,8], but also systemic glucose tolerance and insulin sensitivity. To identify potential mechanisms behind the actions of FXR-deficiency on inflammation and insulin sensitivity in eWAT, differentially expressed genes and pathways were identified by a transcriptomic analysis comparing Ad-FXR$^{-/-}$ and Ad-FXR$^{+/+}$ adipocytes. As expected, inflammatory pathways were down-regulated in Ad-FXR$^{-/-}$ adipocytes, whereas insulin signaling was upregulated, which correlated with the improved insulin sensitivity in Ad-FXR$^{-/-}$ mice after intraperitoneal insulin injection. It is conceivable that the improved WAT insulin sensitivity contributes to the tendency of improved whole-body insulin sensitivity [37]. Whole-body, lean FXR-deficient mice displayed systemic glucose intolerance and peripheral insulin resistance when fed regular chow diets [14], while HFD-fed FXR-deficient mice displayed improved systemic glucose homeostasis [13]. By contrast, transgenic mice overexpressing human FXR in adipocytes driven by the *aP2* promoter showed systemic insulin resistance [36]. These effects are, at least in part, mediated by WAT [24,38], likely involving adipocyte FXR expression, as shown by the results of the *in vitro* experiments [15,39].

Moreover, the transcriptomic analysis showed an upregulation of xenobiotic metabolism in Ad-FXR$^{-/-}$ compared to Ad-FXR$^{+/+}$ adipocytes. The WAT xenobiotic pathway encompasses the glutathione-S-transferase (GST) and cytochrome P450 (CYP) enzyme activities [40,41]. The strongest up-regulated gene in this pathway upon FXR-deficiency encodes *Gsta4*. This anti-oxidant enzyme protects cells from the deleterious effects of α,β-unsaturated aldehydes derived from peroxidized lipids produced during oxidative stress [42]. 4-HNEs are cytotoxic and signaling mediators of oxidative stress leading to protein carbonylation and mitochondrial dysfunction [42]. In WAT, *Gsta4* expression is down-regulated in obesity models, as well as in cultured adipocytes treated with pro-inflammatory cytokines, especially *Tnf*α, leading to an increase in protein carbonylation, reactive oxygen species (ROS) production and mitochondrial dysfunction [20,21].

Our results suggest that FXR inhibits *Gsta4* gene expression. Indeed, *Gsta4* gene expression is upregulated in FXR-deficient adipocytes. Assessment of published liver FXR ChIP-seq data localized a potential FXR response element in the *Gsta4* gene promoter [22], which binds FXR protein in *in vitro* differentiated adipocytes from FXR$^{+/+}$, but not from FXR$^{-/-}$ mice. Based on published data and our results, we propose a model (Figure 7) in which, under obesogenic HFD conditions, locally produced *Tnf*α promotes oxidative stress, inflammation and decreases insulin sensitivity [5,8] in WAT. Adipocyte-specific FXR-deficiency leads to up-regulation of *Gsta4* gene expression, contributing to increased eWAT insulin sensitivity, as well as to improved systemic glucose tolerance and insulin sensitivity [37].

In summary, we identify an unexpected pro-inflammatory function of the nuclear receptor FXR in WAT. This function is, in part, mediated by the decreased expression of the anti-oxidant enzyme *Gsta4* and connected pro-oxidant and inflammatory responses to local insulin resistance and systemic glucose homeostasis.

4. MATERIALS AND METHODS

4.1. *In vivo* studies in mice

Mice were maintained on 12h light/12h dark cycles under controlled environmental conditions with free access to water and food. All experiments were approved by the relevant ethical committee CEEA75 (n° 2015121522544671). C57Bl/6J FXR$^{-/-}$ and wild type (FXR$^{+/+}$) littermate mice have been previously described [17]. C57Bl/6J adipocyte-specific FXR-deficient (Ad-FXR$^{-/-}$) mice (FXR$^{flox/flox}$AdipoQ-Cre$^{+/-}$) were generated by crossing FXR-floxed (FXR$^{flox/flox}$) mice with Adiponectin-Cre recombinase expressing (AdipoQ-Cre$^{+/-}$) mice (Jackson Laboratories, Bar Harbor, USA). 8—10 week old Ad-FXR$^{-/-}$

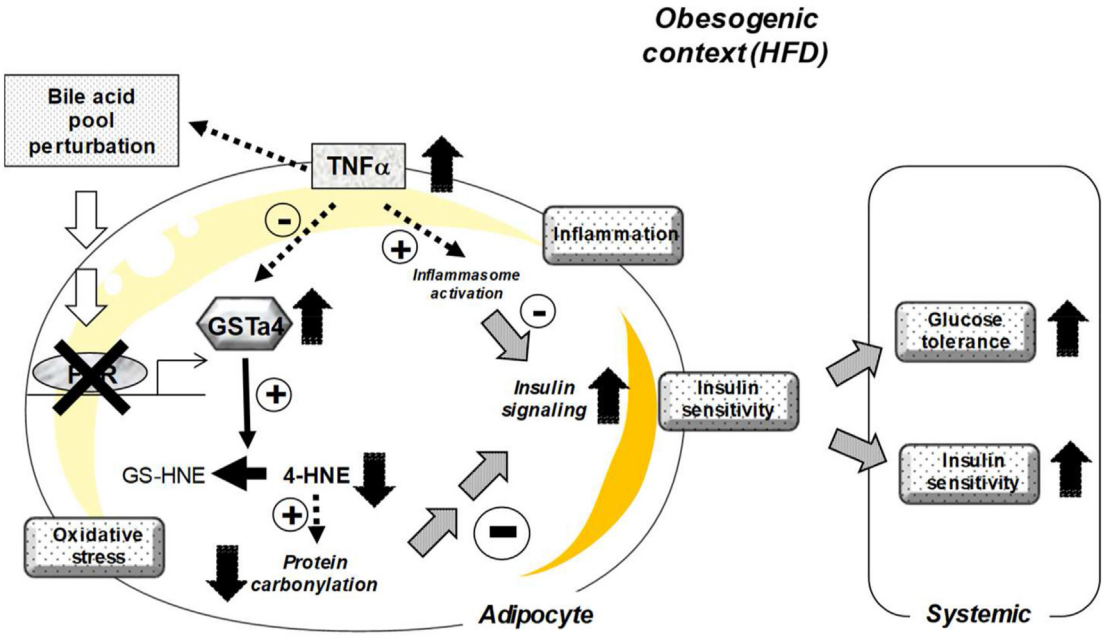

Figure 7: Adipocyte-specific FXR-deficiency increases adipocyte *Gsta4* expression and improves local and systemic glucose homeostasis. HFD-induced obesity results in inflammation, increasing pro-inflammatory TNFalpha production in WAT and leading to decreased adipocyte insulin signaling in the due to both inflammasome activation and oxidative stress (reduced expression of the anti-oxidant enzyme *Gsta4*). Adipocyte-specific FXR-deficiency enhances *Gsta4* expression, leading to increased glutathionylation of lipid aldehydes 4-HNE and protein carbonylation, hence reducing oxidative stress and inflammation. These effects contribute to increased WAT insulin sensitivity and systemic glucose tolerance and insulin sensitivity.

and Ad-FXR$^{+/+}$ littermates (FXR$^{fl/fl}$ genotype) male mice were fed low fat diet (LFD) (10 kcal% fat; Research Diets, New Brunswick, USA), high fat diet (HFD) (60 kcal% fat; Research Diets) for 12 weeks. Weight and fasting glycemia (Accu-Check; Roche Diagnostics, Bâle, Switzerland) were monitored weekly. Serum insulin levels were measured by ELISA (Mouse Insulin ELISA kit; 10-1247-01; Mercodia, Winston Salem, USA). For glucose tolerance (IPGTT) and insulin tolerance (ITT) tests, respectively 1 g/kg of glucose and 0,75UI/kg of insulin were injected intraperitoneally and blood glucose was measured at the indicated times. Epididymal WAT (eWAT) insulin sensitivity was measured after intraperitoneal injection of 1mUI/g insulin in fasting mice. The organs were collected 8min after insulin injection and Western blot analysis were performed.

4.2. Flow cytometry analyses

For stromal vascular fraction (SVF) isolation, eWAT of LFD- and HFD-fed mice was isolated and immediately rinsed in cold Phosphate Buffered Saline (PBS; Life Technologies, Carlsbad, USA). eWAT was then cut in 1-2 mm pieces and digested in Dulbecco modified Eagle's minimal essential medium (DMEM; Life Technologies) supplemented with 0.1% collagenase type I (C2674; Sigma-Aldrich, Saint-Louis, USA) at 37°C for 1h under agitation. Enriched-mature adipocyte cell fraction (floating cells) and SVF cells (pellet) were separated by centrifugation. Immune cells from SVF were characterized by flow cytometry using fluorochrome-conjugated surface protein-specific antibodies (Supp. Figure 2). Macrophages were stained using anti-CD45-BV510 (BLE103138; Biolegend, San Diego, USA), anti-CD11b-BUV395 (563553; BD Biosciences, San Jose, USA), anti-F4/80-PE/Cy7 (BLE123114; Biolegend), anti-CD11c-Percp-Cy5.5 (BLE117328; Biolegend) and anti-CD206-AF647 (BLE141712; Biolegend) antibodies. Cells were analysed using a FORTESSA X20 flow cytometer (Becton Dickinson, New Jersey, USA). Results were acquired using the FACS Diva software (BD Biosciences). Macrophages (CD45^{+} CD11b^{+} F4/80^{+}) from FXR$^{-/-}$ Ad-FXR$^{-/-}$ and littermate mice were isolated using a BD Influx cell sorter (BD Biosciences).

4.3. Western blot and biochemical analyses

Proteins were extracted from cells and tissues using Cell Lysis Buffer (9803, Cell Signaling Technologies, Danvers, USA) and separated by SDS-PAGE. Proteins were detected using antibodies for phospho-Akt (9271S; Cell Signaling Technologies), Akt (92972S; Cell Signaling Technologies), *GSTA4* (Ab134919; Abcam, Cambridge, England), FXR (PP-A9033A-00; RD Systems, Minneapolis, USA) and beta-actin (A5441; Sigma-Aldrich). Staining intensities were quantified using the I-Bright analysis (IBA) software. 4-hydroxy-2-nonenal (4HNE) level was measured using the OxiSelect HNE Adduct competitive ELISA kit according to the manufacturer's instructions (#STA-838; Cell Biolabs, San Diego, USA).

4.4. *In vitro* differentiation of primary adipocytes

eWAT SVF cells, isolated from 10-15 weeks old FXR$^{-/-}$ and FXR$^{+/+}$ female mice as described above, were seeded in DMEM/F12 medium (11320033; Thermo Fisher Scientific, Waltham, USA) supplemented with 10% fetal bovine serum (FBS). Upon reaching confluence, adipocyte differentiation was induced with 0.5 mM IBMX (I5879; Sigma-Aldrich), 2.5 μM dexamethasone (D1756; Sigma-Aldrich), 0.5 μg/ml insulin (I5500; Sigma-Aldrich) and 1 μM rosiglitazone (R2408; Sigma-Aldrich) in DMEM medium. 8 days after confluence, the *in vitro* differentiated adipocytes were treated with *Tnfα* (20 ng/ml) for 6h and 24h.

4.5. RNA extraction and quantitative PCR (qPCR)

Total RNA was isolated from mouse eWAT tissue and cells using Trizol reagent (15596018; ThermoFisher Scientific) and reverse transcribed into cDNA using the High Capacity cDNA reverse transcription kit (4368813; Applied Biosystems, Waltham, USA). Quantitative PCR (qPCR) analysis was performed with the Brilliant II SYBR Green QPCR Master Mix (600831; Agilent Technologies, Santa Clara, USA) on an Mx3005P (Agilent Technologies). Gene expression levels were determined using the ddCt method and normalized to housekeeping gene *18S* (in vivo experiments) and *Cyclophilin A* (*in vivo* experiments) mRNA levels.

4.6. Chromatin-immunoprecipitation (ChIP) experiments

Briefly, 20x10^{6} mature adipocytes were double-crosslinked with 2 mM of Di-(N-Succinimidyl)- Glutarate (DSG; 20593, ThermoFisher Scientific) and 1% formaldehyde (262649, Sigma-Aldrich). After 3 sonication cycles of 10min (30″ ON/30″ OFF), FXR-DNA complexes were immunoprecipitated, washed, eluted, purified and submitted to quantitative PCR analysis [43]. The following oligonucleotide were used: Forward 5′-TCAGGCATGAACCACCATAC3'/Reverse 5′-AACATCCACACGTCCAGTGA-3′ and Forward 5′-AAACATTTTCACATCTAAAGCTTGTTTATTTCCCAAAGAGAAAACGTGGGCTGGGGACGG3'/Reverse 5′- GATCTTTACTTGATCCGCAAACACAGGAGTAAAACCCAGTCGCTTAGCCTTCCATGGTGT-3 were used to amplify respectively negative region (region in the genome that does not show any transcription regulation mark and used to define the background of the experiment) and *Gsta4* gene promoter. Fold enrichments for FXR binding on control region and *Gsta4* gene promoter were calculated using the comparative Ct method and expressed vs input samples.

4.7. Microarray analysis

Enriched-mature adipocyte cell fraction from eWAT of 12 week HFD-fed Ad-FXR$^{-/-}$ and littermate Ad-FXR$^{+/+}$ mice were collected by centrifugation and immediately frozen. RNA was extracted and concentration and integrity number evaluated using the Bioanalyser 2100 (Agilent Biotechnologies). RNA (300 ng) was amplified, fragmented and labelled using the Gene Chip WT Plus Reagent kit (902280, Affymetrix, Santa Clara, USA). Labelled RNA was hybridized to MoGene 2.0 ST gene chips (Affymetrix). Washing and final staining were performed on the Gene Chip Fluidics Station 450 (Affymetrix). DNA chips were scanned using the Gene Chip Scanner 3000 7G (Affymetrix). Microarray data were processed using Galaxy-based Interactive tools for ANalysis of Transcriptomic data (GIANT) [44] on a local instance of Galaxy [45]. Gene set enrichment analyses were performed using the GSEA tool (v.4.0.3) from Broad Institute [46].

4.8. Statistical analysis

All values are expressed as means ± SEM. Statistical significance was analyzed as indicated in figure legends by two-way ANOVA with Tukey *post-hoc* test or with Bonferroni post hoc test when both mouse genotypes and diet effects were analyzed or by student's t-test when only diet effects were analyzed using Prism (GraphPad). Differences were considered significant when $p \leq 0.05$.

AUTHOR CONTRIBUTIONS

H Dehondt: methodology, validation, formal analysis, investigation, resources, writing - original draft; **A Marino:** methodology, validation, formal analysis, investigation, writing - review & editing; **L Butruille:** methodology, validation, formal analysis, investigation, writing - review

& editing; D Mogilenko: conceptualization, supervision, methodology, validation, formal analysis, investigation, writing - review & editing; **AC Nzoussi Loubota:** investigation; **O Chavez-Talavera:** investigation, writing - review & editing; **E Dorchies:** investigation, ressources; **E Vallez:** investigation, ressources; **J Haas:** formal analysis, writing - review & editing; **B Derudas:** investigation; **A Bongiovanni:** investigation; **M Tardivel:** investigation; **F Kuipers:** writing - review & editing; **P Lefebvre:** writing - review & editing; **S Lestavel:** writing - review & editing; **A Tailleux:** writing - review & editing; **D Dombrowicz:** supervision, writing - original draft, project administration, funding acquisition; **S Caron:** conceptualization, supervision, methodology, validation, formal analysis, investigation, resources, writing - original draft, project administration, funding acquisition; **B Staels:**. Supervision, writing - original draft, writing - review & editing, project administration, funding acquisition.

FUNDING

The authors' research work was supported by grants from Agence Nationale pour la Recherche (ANR FXRen and ANR-10-LABX-46) and the European Union (FP6 Hepadip FP6-018734; FP7 Resolve FP7-305707). B.S. is a recipient of an Advanced ERC Grant (694717).

DATA AVAILABILITY

Data will be made available on request.

ACKNOWLEDGEMENTS

We thank Sarah Gabut (US 41 - UAR 2014 — PLBS, Univ. Lille, CNRS, Inserm, CHU Lille, Institut Pasteur de Lille) for her assistance with the histology analysis.

CONFLICT OF INTEREST

The authors have no conflict of interest to declare.

APPENDIX A. SUPPLEMENTARY DATA

Supplementary data to this article can be found online at https://doi.org/10.1016/j.molmet.2023.101686.

REFERENCES

[1] NCD Risk Factor Collaboration (NCD-RisC). Trends in adult body-mass index in 200 countries from 1975 to 2014: a pooled analysis of 1698 population-based measurement studies with 19.2 million participants. Lancet 2016;387:1377—96. https://doi: 10.1016/S0140-6736(16)30054-X.

[2] Reilly SM, Saltiel AR. Adapting to obesity with adipose tissue inflammation. Nat Rev Endocrinol 2017;13:633—43. https://doi: 10.1038/nrendo.2017.90.

[3] Vishvanath L, Gupta RK. Contribution of adipogenesis to healthy adipose tissue expansion in obesity. J Clin Invest 2019;129:4022—31. https://doi: 10.1172/JCI129191.

[4] Hruskova Z, Biswas SKA. New "immunological" role for adipocytes in obesity. Cell Metabol 2013;17:315—7. https://doi: 10.1016/j.cmet.2013.02.015.

[5] Hotamisligil GS, Peraldi P, Budavari A, Ellis R, White MF, Spiegelman BM. IRS-1-mediated inhibition of insulin receptor tyrosine kinase activity in TNF-alpha- and obesity-induced insulin resistance. Science 1996;271:665—8. https://doi: 10.1126/science.271.5249.665.

[6] Biswas SK, Mantovani A. Orchestration of metabolism by macrophages. Cell Metab 2012;15:432—7. https://doi: 10.1016/j.cmet.2011.11.013.

[7] Nishimura S, Manabe I, Nagasaki M, Eto K, Yamashita H, Ohsugi M, et al. CD8+ effector T cells contribute to macrophage recruitment and adipose tissue inflammation in obesity. Nat Med 2009;15:914—20. https://doi: 10.1038/nm.1964.

[8] Hotamisligil GS, Shargill NS, Spiegelman BM. Adipose expression of tumor necrosis factor-alpha: direct role in obesity-linked insulin resistance. Science 1993;259:87—91. https://doi: 10.1126/science.7678183.

[9] Prawitt J, Caron S, Staels B. Glucose-lowering effects of intestinal bile acid sequestration through enhancement of splanchnic glucose utilization. Trends Endocrinol. Metab 2014;25:235—44. https://doi: 10.1016/j.tem.2014.03.007.

[10] Chavez-Talavera O, Haas J, Grzych G, Tailleux A, Staels B. Bile acid alterations in nonalcoholic fatty liver disease, obesity, insulin resistance and type 2 diabetes: what do the human studies tell? Curr Opin Lipidol 2019;30:244—54. https://doi: 10.1097/MOL.0000000000000597.

[11] Mazuy C, Helleboid A, Staels B, Lefebvre P. Nuclear bile acid signaling through the farnesoid X receptor. Cell Mol Life Sci 2015;72:1631—50. https://doi: 10.1007/s00018-014-1805-y.

[12] Molinaro A, Wahlström A, Marschall HU. Role of Bile Acids in Metabolic Control. Trends Endocrinol. Metab 2018;29:31—41. https://doi: 10.1016/j.tem.2017.11.002.

[13] Prawitt J, Abdelkarim M, Stroeve JH, Popescu I, Duez H, Velagapudi VR, et al. Farnesoid X receptor deficiency improves glucose homeostasis in mouse models of obesity. Diabetes 2011;60:1861—71. https://doi: 10.2337/db11-0030.

[14] Cariou B, van Harmelen K, Duran-Sandoval D, van Dijk TH, Grefhorst A, Abdelkarim M, et al. The farnesoid X receptor modulates adiposity and peripheral insulin sensitivity in mice. J Biol Chem 2006;281:11039—49. https://doi: 10.1074/jbc.M510258200.

[15] Rizzo G, Disante M, Mencarelli A, Renga B, Gioiello A, Pellicciari R, et al. The farnesoid X receptor promotes adipocyte differentiation and regulates adipose cell function in vivo. Mol. Pharmacol 2006;70:1164—73. https://doi: 10.1124/mol.106.023820.

[16] Abdelkarim M, Caron S, Duhem C, Prawitt J, Dumont J, Lucas A, et al. The farnesoid X receptor regulates adipocyte differentiation and function by promoting peroxisome proliferator-activated receptor-gamma and interfering with the Wnt/beta-catenin pathways. J Biol Chem 2010;285:36759—67. https://doi: 10.1074/jbc.M110.166231.

[17] Sinal CJ, Tohkin M, Miyata M, Ward JM, Lambert G, Gonzalez FJ. Targeted disruption of the nuclear receptor FXR/BAR impairs bile acid and lipid homeostasis. Cell 2000;102:731—44. https://doi: 10.1016/s0092-8674(00)00062-3.

[18] Lee KY, Russell SJ, Ussar S, Boucher J, Vernochet C, Mori MA, et al. Lessons on conditional gene targeting in mouse adipose tissue. Diabetes 2013;62:864—74. https://doi: 10.2337/db12-1089.

[19] He NG, Singhal SS, Srivastava SK, Zimniak P, Awasthi YC, Awasthi S. Transfection of a 4-hydroxynonenal metabolizing glutathione S-transferase isozyme, mouse *GSTA4*-4, confers doxorubicin resistance to Chinese hamster ovary cells. Arch Biochem Biophys 1996;333:214—20. https://doi: 10.1006/abbi.1996.0383.

[20] Curtis JM, Grimsrud PA, Wright WS, Xu X, Foncea RE, Graham DW, et al. Downregulation of adipose glutathione S-transferase A4 leads to increased protein carbonylation, oxidative stress, and mitochondrial dysfunction. Diabetes 2010;59:1132—42. https://doi: 10.2337/db09-1105.

[21] Curtis JM, Hahn WS, Stone MD, Inda JJ, Droullard DJ, Kuzmicic JP, et al. Protein carbonylation and adipocyte mitochondrial function. J Biol Chem 2012;287:32967—80. https://doi: 10.1074/jbc.M112.400663.

[22] Thomas AM, Hart SN, Kong B, Fang J, Zhong XB, Guo GL. Genome-wide tissue-specific farnesoid X receptor binding in mouse liver and intestine. Hepatology 2010;51:1410—9. https://doi: 10.1002/hep.23450.

[24] Shihabudeen MS, Roy D, James J, Thirumurugan K. Chenodeoxycholic acid, an endogenous FXR ligand alters adipokines and reverses insulin resistance. Mol Cell Endocrinol 2015;414:19—28. https://doi: 10.1016/j.mce.2015.07.012.

[25] Yao J, Zhou CS, Ma X, Fu BQ, Tao LS, Chen M, et al. FXR agonist GW4064 alleviates endotoxin-induced hepatic inflammation by repressing macrophage activation. World J. Gastroenterol 2014;20:14430–41. https://doi:10.3748/wjg.v20.i39.14430.

[26] Mudaliar S, Henry R, Sanyal AJ, Morrow L, Marschall AU, Kipnes M, et al. Efficacy and safety of the farnesoid X receptor agonist obeticholic acid in patients with type 2 diabetes and nonalcoholic fatty liver disease. Gastroenterology 2013;145:574–82. https://doi: 10.1053/j.gastro.2013.05.042.

[27] Schwabl P, Hambruch E, Seeland BA, Hayden H, Wagner M, Garnys L, et al. The FXR agonist PX20606 ameliorates portal hypertension by targeting vascular remodelling and sinusoidal dysfunction. J Hepatol 2017;66:724–33. https://doi: 10.1016/j.jhep.2016.12.005.

[28] Hao H, Cao L, Jiang C, Che Y, Zhang S, Takahashi S, et al. Farnesoid X Receptor Regulation of the NLRP3 Inflammasome Underlies Cholestasis-Associated Sepsis. Cell Metab 2017;25:856–67. https://doi: 10.1016/j.cmet.2017.03.007.

[29] Gadaleta RM, van Erpecum KJ, Oldenburg B, Willemsen EC, Renooij W, Murzilli S, et al. Farnesoid X receptor activation inhibits inflammation and preserves the intestinal barrier in inflammatory bowel disease. Gut 2011;60:463–72. https://doi: 10.1136/gut.2010.212159.

[30] Fang S, Suh JM, Reilly SM, Yu E, Osborn O, Lackey D, et al. Intestinal FXR agonism promotes adipose tissue browning and reduces obesity and insulin resistance. Nat Med 2015;21:159–65. https://doi: 10.1038/nm.3760.

[31] Miyazaki T, Shirakami Y, Mizutani T, Maruta A, Ideta T, Kubota M, et al. Novel FXR agonist nelumal A suppresses colitis and inflammation-related colorectal carcinogenesis. Sci Rep 2021;11:492. https://doi: 10.1038/s41598-020-79916-5.

[32] Lian F, Xing X, Yuan G, Schäfer C, Rauser S, Walch A, et al. Farnesoid X receptor protects human and murine gastric epithelial cells against inflammation-induced damage. Biochem. J. 2011;438:315–23. https://doi: 10.1042/BJ20102096.

[33] Renga B, Migliorati M, Mencarelli A, Fiorucci S. Reciprocal regulation of the bile acid-activated receptor FXR and the interferon-gamma-STAT-1 pathway in macrophages. Biochim. Biophys. Acta. 2009;1792:564–73. https://doi: 10.1016/j.bbadis.2009.04.004.

[34] Kloting N, Bluher M. Adipocyte dysfunction, inflammation and metabolic syndrome. Rev Endocr Metab Disord 2014:277–87. https://doi: 10.1007/s11154-014-9301-0.

[35] Blaszczak AM, Jalilvand A, Hsueh WA. Adipocytes, innate immunity and obesity: a mini-review. Front Immunol 2021;12:650768. https://doi: 10.3389/fimmu.2021.650768.

[36] van Zutphen T, Stroeve JHM, Yang J, Bloks VW, Jurdzinski A, Roelofsen H, et al. FXR overexpression alters adipose tissue architecture in mice and limits its storage capacity leading to metabolic derangements. J Lipid Res 2019;60:1547–61. https://doi: 10.1194/jlr.M094508.

[37] Morley TS, Xia JY, Scherer PE. Selective enhancement of insulin sensitivity in the mature adipocyte is sufficient for systemic metabolic improvements. Nat Commun 2015;6:7906. https://doi: 10.1038/ncomms8906.

[38] Maneschi E, Vignozzi L, Morelli A, Mello T, Filippi S, Cellai I, et al. FXR activation normalizes insulin sensitivity in visceral preadipocytes of a rabbit model of MetS. J. Endocrinol 2013;218:215–31. https://doi: 10.1530/JOE-13-0109.

[39] Tao J, Yu XL, Yuan YJ, Shen X, Liu J, Gu PP, et al. DMRT2 Interacts With FXR and Improves Insulin Resistance in Adipocytes and a Mouse Model. Front. Endocrinol. (Lausanne) 2022;12:723623. https://doi: 10.3389/fendo.2021.723623.

[40] Coles BF, Kadlubar FF. Human alpha class glutathione S-transferases: genetic polymorphism, expression, and susceptibility to disease. Methods Enzymol 2005;401:9–42. https://doi: 10.1016/S0076-6879(05)01002-5.

[41] Ellero S, Chakhtoura G, Barreau C, Langouët S, Benelli C, Penicaud L, et al. Xenobiotic-metabolizing cytochromes p450 in human white adipose tissue: expression and induction. Drug Metab. Dispos 2010;38:679–86. https://doi: 10.1124/dmd.109.029249.

[42] Awasthi YC, Ramana KV, Chaudhary P, Srivastava SK, Awasthi S. Regulatory roles of glutathione-S-transferases and 4-hydroxynonenal in stress-mediated signaling and toxicity. Free Radic Biol Med 2017;111:235–43. https://doi: 10.1016/j.freeradbiomed.2016.10.493.

[43] Caron S, Huaman Samanez C, Dehondt H, Ploton M, Briand O, Lien F, et al. Farnesoid X receptor inhibits the transcriptional activity of carbohydrate response element binding protein in human hepatocytes. Mol. Cell Biol 2013;33:2202–11. https://doi: 10.1128/MCB.01004-12.

[44] Vandel J, Gheeraert C, Staels B, Eeckhoute J, Lefebvre P, Dubois-Chevalier J. GIANT: galaxy-based tool for interactive analysis of transcriptomic data. Sci. Rep. 2020;10:19835. https://doi: 10.1038/s41598-020-76769-w.

[45] Afgan E, Baker D, Batut B, van den Beek M, Bouvier D, Cech M, et al. The Galaxy platform for accessible, reproducible and collaborative biomedical analyses: 2018 update. Nucleic Acids Res 2018;46:W537–44. https://doi: 10.1093/nar/gky379.

[46] Subramanian A, Tamayo P, Mootha VK, Mukherjee S, Ebert BL, Gillette MA, et al. Gene set enrichment analysis: a knowledge-based approach for interpreting genome-wide expression profiles. Proc. Natl. Acad. Sci. U S A 2005;102:15545–50. https://doi: 10.1073/pnas.0506580102.

